

LOW CYCLE FATIGUE BEHAVIOR OF DP980 STEEL GAS METAL ARC WELDING JOINTS

JULIANA GUADALUPE ROSADO-CARRASCO^{1,2}, WALTER FRANCISCO GONZALEZ-ZAPATERO¹, RICARDO R. AMBRIZ¹, DAVID JARAMILLO¹

1. Instituto Politécnico Nacional CIITEC-IPN, Cerrada de Cecati S/N Col. Sta. Catarina, Azcapotzalco, Ciudad de México
2. Instituto Politécnico Nacional ESIQIE-IPN, Av. Instituto Politécnico Nacional, Lindavista, Gustavo A. Madero, Ciudad de México

Dual phase (DP) steels, which are widely used in automotive industry, have a good balance between high strength and ductility. These capacities are reached due to a perfect phase combination in the DP microstructures. However, automotive parts manufactured with DP steel are often joined by arc welding processes, which generates a heat affected zone. In addition, during service, the components are subjected to cyclic loadings that can exceed the yield strength locally (besides the geometry of the component). In this work, 1.6 mm-thick DP980 steel sheets were welded by gas metal arc welding process to analyze the low cycle fatigue behavior. The tests were conducted under a constant amplitude strain control mode. The welded joints experienced a fatigue life reduction with respect to the DP980 steel of ~16% at strain amplitudes of 0.2, 0.3, and 0.4%. For strain amplitudes larger than 0.6%. The fatigue life of the welded joint was reduced by 39%.

Keywords: DP980 steel sheet; low cycle fatigue; gas metal arc welding; heat affected zone; tempered martensite

Introduction. Advanced High-Strength Steels (AHSS) is a group of steels widely used by the automotive industry because of their superior mechanical properties obtained by well-controlled thermomechanical processes and the resulting microstructures. Dual-Phase (DP) steels are part of this group. DP steel's microstructure consists of a ferrite matrix (α) with dispersed martensite islands [1–3]. Due to their high formability, the DP steels (and all the AHSS group) are suitable to fabricate lighter components with smaller thickness, reducing the final weight of the automotive body structure [4–6].

The automotive industry requires electric arc welding processes to join several components of the car body structures, and these joining processes produce a heat input that modifies the distribution and morphology of the martensite and ferrite grain size in the DP steels. Thus, the final behavior and durability of the welded components are modified [7]. Gas Metal Arc Welding (GMAW) is a permanent joining process by electric arc and filler metal, which is applied on automotive body structures, where the Resistance Spot Welding (RSW) cannot be used, such as in butt joints [7,8]. The electric arc induces a Heat Affected Zone (HAZ) in the material region adjacent to the Fusion Zone (FZ) [7, 9].

Unfortunately, there is a lack of studies in the literature where DP welded joints are subjected to low cycle fatigue (LCF) conditions, and the soft zone is evaluated under these service conditions. Awareness of the softened zone induced in electric arc welded joints of DP steels and the related loss of mechanical strength under monotonic loading condition is of relevance for automotive body design. Furthermore, the fatigue response of the HAZ under LCF conditions is extremely relevant. For these reasons, this research work focuses on the analysis of GMAW welded joints of DP980 steel subjected to monotonic and cyclic loading conditions which generate cyclic plastic strains. The welded joints were evaluated by microstructural and hardness analysis. Fatigue behavior is also reported in terms of cyclic strain hysteresis loops, cyclic stress-strain curves, variable stress amplitude response during the cyclic loads, strain-life, and stress-life curves.

Materials and methods. DP980 steel sheets with dimensions of 280mm x 140mm x 1.60mm were joined using a standard flare V-groove configuration in agreement with the standard AWS D9.1 [10], as showed in Figure 1a. To obtain the joints, the GMAW process was performed using a Miller® Dimension 652 power source (Miller Electric Mfg. LLC., Appleton, WI, USA) equipped with a control panel, wire feeder, and a welding torch. A semiautomatic device implemented by the working group (CIITEC, Mexico City, Mexico) was used to keep a constant welding speed and a straight path. Shielding gas consisting of a mixture of 20% CO₂ and 80% Ar (volume fraction) was used at a flow rate of 0.03 mm³min⁻¹. The used welding parameters were a V voltage of 20 V, I current of 90 A, v travel speed of 5 mm s⁻¹ and a pre-heating temperature of 240 °C. According to Equation (1), a heat input Q of 302 J mm⁻¹ was determined considering a thermal efficiency η of 84% for the GMAW process [11]. In addition, K-type thermocouples were placed on the welding plate (at distances of 4 mm and 5.5 mm from the weld center) to obtain temperature measurements in the HAZ. Figure 1b shows the experimental setup for the welding process and the K-type thermocouples attached to the plate, which were connected to a data acquisition card from National Instruments model 913. An insulator ceramic was used to protect the thermocouple sensors from the electric arc.

$$Q = \eta \frac{VI}{v} \quad (1)$$

Results and discussion. The cyclic stable response in terms of true stress vs. strain for the DP980 steel sheet and welded joint is presented in Figure 2a, b. Comparing Figure 2a, b, the DP980 steel sheet exhibited a slender hysteresis loop for 0.006 and 0.008 strain amplitudes. Thus, the plastic strain was higher for the welded joint subjected to high strain amplitudes under cyclic stable response. In the case of strain amplitudes equal to 0.004 or smaller, both materials presented narrow hysteresis loops, with just a small difference between the DP980 and welded joint. The welded joint exhibited the slender hysteresis loops, which

apparently indicated a smaller plastic strain than in the DP980 steel. However, the hysteresis loops correspond to the cyclic stable response of the materials, and the welded joint could not present the smaller plastic strains.

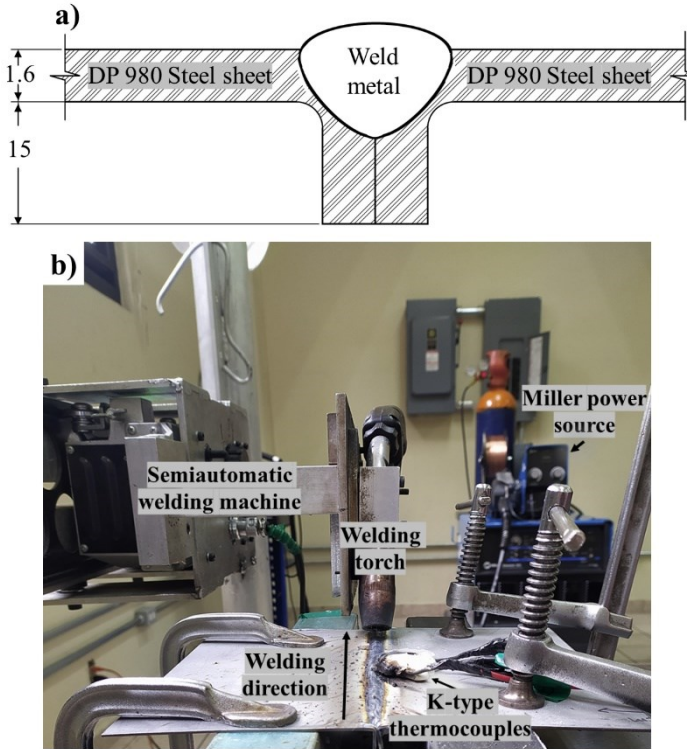


Fig. 1. Configuration for welding process of DP980 steel sheets (a) Schematic draw for the joint geometry with a standard flare V-groove preparation, dimensions are in mm. (b) Experimental setup.

Table 1 presents the LCF test program used for the DP980 and welded joints, which consists of five different strain amplitudes ϵ_a and test frequencies.

Strain amplitude, ϵ_a (%)	Test frequency, f (Hz)
0.2	2
0.3	1.333
0.4	1
0.6	0.667
0.8	0.5

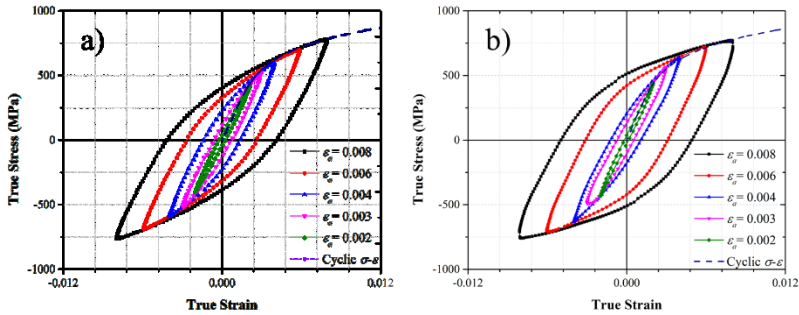


Fig. 2. Hysteresis loops in LCF corresponding to (a) DP980 steel sheet and (b) welded joints.

Figure 3a, b showed that for the applied strain amplitudes, the welded joint presented the larger plastic strains. This result was not clear from the previously presented hysteresis loops in Figure 2a, b, but it can be explained based on the yield strength of the materials. The welded joint presented a lower yield strength, which can be associated with the tempered martensite in the Low Temperature Heat Affected Zone (LT-HAZ) of the welded joint and is a result of the weld thermal cycles. A lower yield strength resulted in the plastic strain arising early for the welded joint. The tempered martensite also induced a softening mechanism, which consists of the coarsening of martensite laths and a decrease of the dislocation density that reduces the movement of the dislocations. These phenomena have been previously reported in the literature [12]. For completeness, Stress vs Number of cycles (S-N) curves for the DP980 steel sheet and welded joint deduced from the LCF tests are presented in Figure 3c,d. Failure of fatigue samples took place at the LT-HAZ, since at this area, the tempered martensite requires the lowest stress to be deformed in the welded joint compared to the other martensite types located in the Fusion Zone (FZ) and the High-Temperature Heat Affected Zone (HT-HAZ) [13].

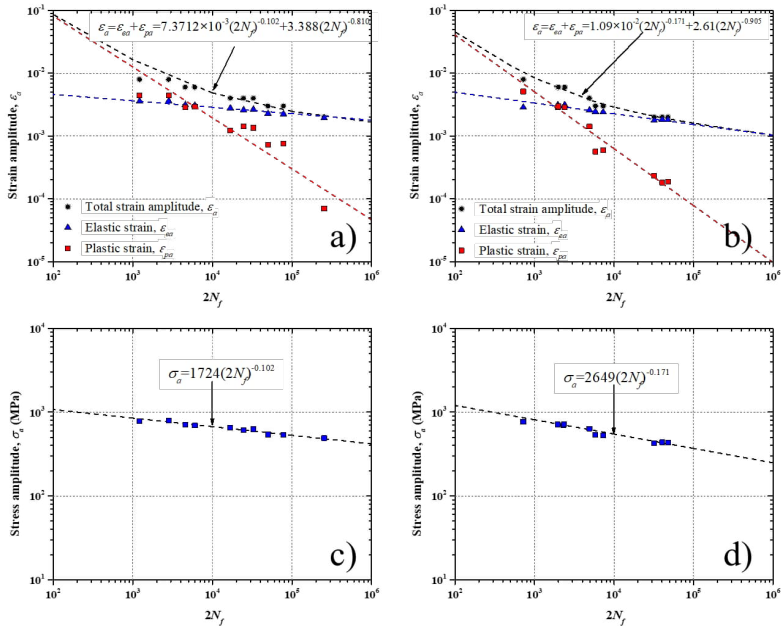


Fig. 3. Total strain vs. $2Nf$. (a) DP980 steel sheet and (b) welded joints. S-N curves of (c) DP980 steel sheet and (d) welded joints.

Conclusions. The main conclusions of this research work are the following:

Dual phase sheet steel of 1.6 mm-thick with a nominal tensile strength of 980 MPa were properly welded by the GMAW process using a heat input of 302 Jmm⁻¹.

Regarding the low cycle fatigue behavior, the strain-cycle data showed a reduced fatigue life for the welded joint compared to the dual-phase steel due to larger plastic strain amplitudes induced in the welded joint.

On average, the fatigue life of the welded joint was reduced by 39% at strain amplitude of 0.6%.

The fatigue life of the welded joint was reduced by 16% for the strain amplitudes of 0.2, 0.3, and 0.4%.

1. Keeler S.; Kimchi M. *Advanced high-strength steels application guidelines version 6.0* // World AutoSteel: Brussels, Belgium. – 2014. – 6. – P. 511.
2. Fonstein N. *Dual-Phase Steels in Automotive Steels* // Elsevier: Amsterdam, The Netherlands. – 2017. – P. 169–216. <https://doi.org/10.1016/B978-0-08-100638-2.00007-9>

3. Davies R.G. Influence of martensite composition and content on the properties of dual phase steels // *Met. Mater. Trans. A.* – 1978. – 9. – P. 671–679. <https://doi.org/10.1007/BF02659924>
4. Dai J., Meng Q., Zheng H. High-strength dual-phase steel produced through fast-heating annealing method // *Results Mater.* – 2020. – 5. – № 100069. <https://doi.org/10.1016/j.rinma.2020.100069>
5. Tasan C., Diehl M., Yan D., Bechtold M., Roters F., Schemmann L., Zheng C., Peranio N., Ponge D., Koyama M., Tsuzaki K., Raabel D. An overview of dual-phase steels: Advances in microstructure-oriented processing and micromechanically guided design // *Annu. Rev. Mater. Sci.* – 2015. – 45. – P. 391–431. <https://doi.org/10.1146/annurev-matsci-070214-021103>
6. Kuziak R., Kawalla R., Waengler S. Advanced high strength steels for automotive industry // *Arch. Civ. Mech. Eng.* – 2008. – 8. – P. 103–117. [https://doi.org/10.1016/S1644-9665\(12\)60197-6](https://doi.org/10.1016/S1644-9665(12)60197-6)
7. Ramazani A., Mukherjee K., Abdurakhmanov A., Prah U., Schleser M., Reisgen U., Bleck W. Micro-macro-characterisation and modelling of mechanical properties of gas metal arc welded (GMAW) DP600 steel // *Mater. Sci. Eng. A.* – 2014. – 589. – P. 1–14. <https://doi.org/10.1016/j.msea.2013.09.056>
8. Ahiale G.K., Oh Y.-J. Microstructure and fatigue performance of butt-welded joints in advanced high-strength steels // *Mater. Sci. Eng. A.* – 2014. – 597. – P. 342–348. <https://doi.org/10.1016/j.msea.2014.01.007>
9. Easterling K. Chapter 1 – Fusion welding – process variables In: *Introduction to the Physical Metallurgy of Welding* // Elsevier Ltd.: Amsterdam, The Netherlands. – 2013. – P. 1–54. <https://doi.org/10.1016/B978-0-7506-0394-2.50006-X>
10. AWS D9 Committee on Welding, Brazing, and Soldering of Sheet Metal // D9.1/D9.1M:2000 Sheet Metal Welding Code. 2000. Available online: <https://www.aws.org/standards/committee/d9-committee-on-sheet-metal-welding-2> (accessed on 1 December 2021).
11. Dupont J.N., Marder A.R. Thermal efficiency of arc welding processes // *Weld. J.* – 1995. – 74. – P. 406–416.
12. Saha D., Biro E., Gerlich A., Zhou Y. Martensite tempering kinetics: Effects of dislocation density and heating rates // *Mater. Charact.* – 2020. – 168. – № 110564. <https://doi.org/10.1016/j.matchar.2020.110564>
13. Sankaran S., Sarma V.S., Padmanabhan K.A. Low cycle fatigue behavior of a multiphase microalloyed medium carbon steel: Comparison between ferrite-pearlite and quenched and tempered microstructures // *Mater. Sci. Eng. A.* – 2003. – 345. – P. 328–335. [https://doi.org/10.1016/S0921-5093\(02\)00511-7](https://doi.org/10.1016/S0921-5093(02)00511-7)